IEEE Access
Multidisciplinary : Rapid Review : Open Access Journal

Received May 16, 2017, accepted June 3, 2017, date of publication June 13, 2017, date of current version July 7, 2017.

Digital Object Identifier 10.1109/ACCESS.2017.2715065

Symmetrical Shoot-Through Based Decoupled Control of Z-Source Inverter

SUMANT G. KADWANE[1], (Senior Member, IEEE), UMESH K. SHINDE[2], (Member, IEEE), SNEHAL P. GAWANDE[1], (Member, IEEE), AND RITESH KUMAR KESHRI[3], (Senior Member, IEEE)
[1]Yeshwantrao Chavan College of Engineering, Nagpur 441110, India
[2]Bhivarabai Sawant College of Engineering and Research, Pune 411041, India
[3]Visvesvaraya National Institute of Technology, Nagpur 440010, India

Corresponding author: Umesh K. Shinde (ukshinde@yahoo.com)

ABSTRACT Total harmonic distortion, produced with the existing PWM techniques for a Z-source inverter topology, is higher due to the unsymmetrical shoot-through, if separate controls of ac and dc sides are required. This paper proposes the concept of symmetrical shoot-through-based modulation and compares the performance with the case of the popular simple boost control. The proposed modulation method achieves a sinusoidal and symmetrical distribution of shoot-through states. This ensures an improved current and voltage profile at the output, along with the capability of decoupled control for the shoot-through and the modulation index control. The effectiveness of the proposed method has been demonstrated and validated through analysis, simulation, and experimentation. This concept can be applied to all the variants of Z-source-based power conversions.

INDEX TERMS Z-source inverter, pulse width modulation, symmetrical shoot-through, and total harmonic distortion.

I. INTRODUCTION

Z-source inverter utilizes, the shoot-through state to boost the inverter output voltage with an added impedance network in cascade with the Voltage Source Inverter (VSI). The advantages of a Z-source inverter over traditional voltage source inverters, and current source inverters have been well demonstrated in the literature. The ZSI is more reliable owing to, the conversion of dead time required in conventional inverters to shoot-through states [1]. The possible shoot-through regions are elaborated in this paper. Extensive PWM techniques have been reported in the literature, and these are well established and widely, used. Among such techniques simple boost control, maximum boost control, constant boost control, and extended boost is commonly used, and have been presented in [1]–[3] with the specific advantages of one technique over the other. For example, maximum boost control is presented to provide a maximum boost or a voltage gain with a certain modulation index. The modifications in the Z-source network have been carried out for the improvements in various parameters like reduced voltage stress, suppressing inrush current surge, and achieve minimum current ripple, etc. with the use of the above PWM methods [4], [5]. The Z-source network is also increasingly, used for various applications of inverters in traction drives of fuel cells, uninterruptable power supplies, electric and hybrid vehicles, distributed generation systems, grid-connected systems, flexible AC transmission systems, and many other practical applications [6]–[10]. Modeling and design procedures for a Z-source impedance network for single phase and three phase applications have been presented in, the literature [11]–[14]. Also, the control strategies for various applications, particularly, regulating the capacitor voltage, output voltage, load current, and inductor current of the ZSI have been analyzed and reported [15]–[18]. The current mode controller is extensively used in most Z-source based topologies like all the other control techniques. All the existing literature uses an unsymmetrical PWM pattern. A different PWM technique, which can provide higher gain with a higher voltage is discussed in [19]. A novel switched boost inverter topology, with a lower number of passive elements is presented in [20]. However, even here, the generation of PWM signals, is unsymmetrical and discontinuous.

Although comprehensive modeling, impedance design, and the control strategies of Z-source based inverters have been extensively carried out, less attention is given to the harmonic analysis of this converter, which is one of the most important aspects of the design of any system. In order, to reduce harmonics in ZSI, harmonic injection methods, which are common in the use of inverter applications have been discussed in previous papers. Despite this, the sine PWM (SPWM) pattern, which is symmetrical by its nature, is labeled asymmetric due to the addition of a shoot-through state, which generates lower order harmonics. This asymmetry is on account of the fact that, the shoot-through states are not introduced in the sinusoidal reference, but are superimposed externally, in non-sinusoidal fashion.

In this paper, the authors have introduced, the concept of Symmetrical Shoot-Through based PWM, in which sinusoidal shoot-through state preserves the sinusoidal nature of the SPWM that, in turn, reduces the THD, of the voltage waveform at the output. So far, the concept of SPWM has never been analyzed in the literature. This suppresses, the lower order harmonics in the waveform, and the higher order harmonics at the output can be eliminated by passive filters, lowering the overall THD of the output. Additionally, decoupled control ensures nearly independent control of the DC side controller and AC side controller. In most of the applications like Photo Voltaic power generation, the DC side controller is used to obtain the maximum power point. The AC side controller is used to regulate and fed the necessary power to the grid.

This paper is organized as: Section II provides the review of mathematical modeling of a Z-source inverter. Section III & IV explain the concept of SST based PWM and control strategy. Section V provides the simulation results and discussion on the improvement in a harmonic profile. Section VI details the experimental setup and hardware results followed by the conclusion in Section VII.

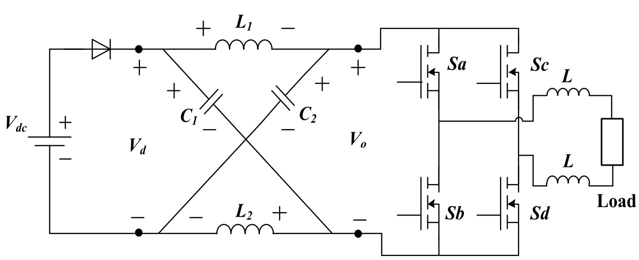

FIGURE 1. Structure of a Z-source Inverter.

II. MATHEMATICAL MODELING OF ZSI

Fig. 1 shows the structure of the ZSI. For ZSI, the output voltage of a Z-source impedance network V_o, and the other parameters as derived in [1] are as follows.

$$V_o = \frac{1-D}{1-2D} V_{dc} \tag{1}$$

Where V_{dc} is the DC source input, T_s is shoot-through duty period, T is the total time period of PWM waveform, and $D = T_s/T$ is the shoot-through duty ratio. In case of Simple Boost Control (SBC), duty ratio is related to modulation index M as

$$D = 1 - M \tag{2}$$

The boost factor B can also be derived as

$$B = \frac{1}{1-2D} \geq 1 \tag{3}$$

From (2) & (3), the boost factor in terms of M can be given as

$$B = \frac{1}{2M-1} \tag{4}$$

The overall gain G is expressed as

$$G = \frac{M}{2M-1} = MB \tag{5}$$

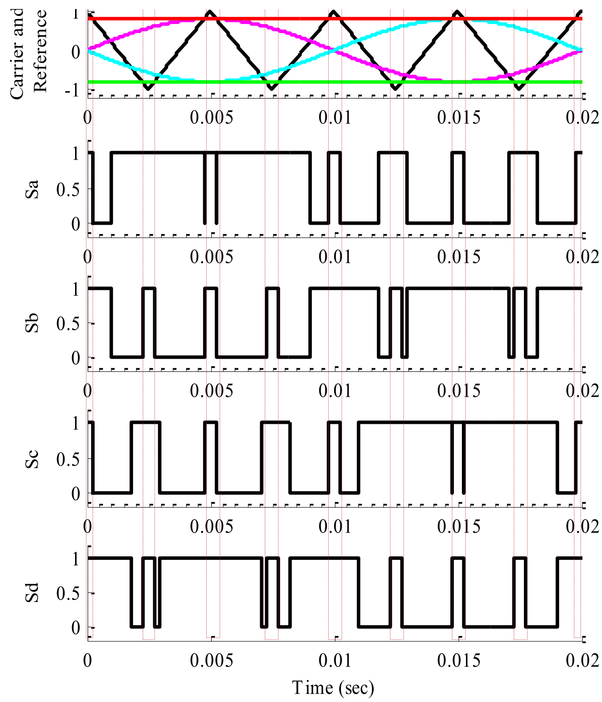

FIGURE 2. Waveform of Simple Boost Control PWM.

III. CONCEPT OF SYMMETRICAL SHOOT-THROUGH BASED PWM

Modulation waveforms of the conventional SBC based control method shown in Fig. 2 have a limitation, as SBC does not add shoot-through states symmetrically, at each pulse of SPWM. Therefore, the sinusoidal nature is not preserved. In order to preserve, the sinusoidal nature of SPWM, it is essential to maintain this symmetry in each pulse of SPWM. The constant shoot-through is inserted symmetrically, at each pulse of SPWM, as shown in Fig. 3. The figure shows that the sinusoidal pattern is preserved in the upper and lower switch for one leg of the H-bridge inverter along with an inserted shoot-through states.

Fig. 4(a), shows the concept of symmetry, in SST. From the figure, it is clear that the shoot-through states are symmetrically distributed across the two sides of the active state.

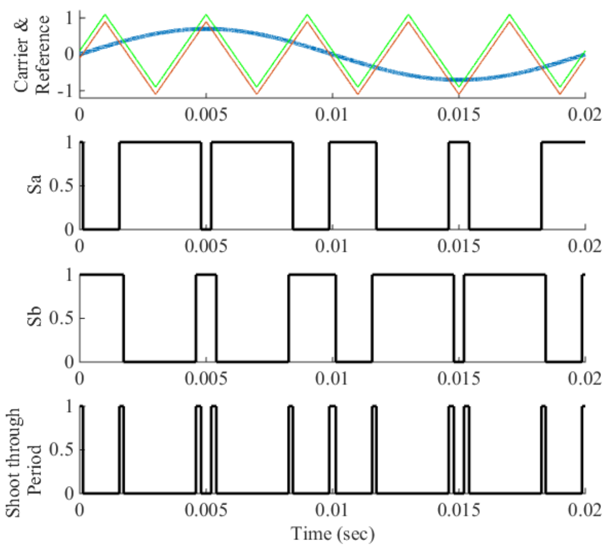

FIGURE 3. Waveform of SST showing sinusoidal pattern and shoot-through states.

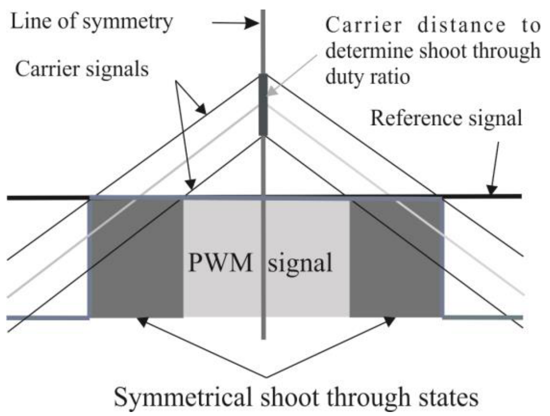

(a)

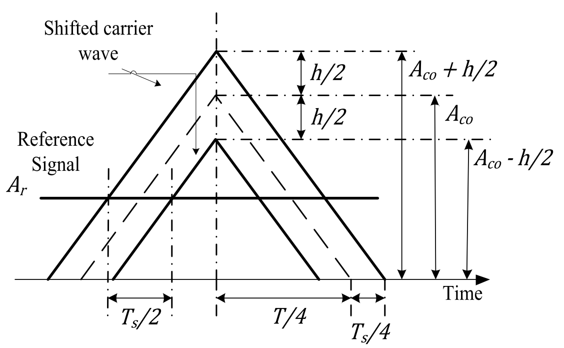

(b)

FIGURE 4. Waveform of SST for mathematical analysis.

These active states are sinusoidally distributed, and therefore, the overall symmetry and sinusoidal pattern are preserved. The analysis of the mathematical model is represented in Fig. 4(b). From the concept of similar triangle,

$$\frac{A_{co}}{T/4} = \frac{h}{T_s/2} \tag{6}$$

Where, A_{co} is the amplitude of the carrier wave, and h is the overall amplitude shift in the upper and lower carrier waves. Rearrangement of (6) for h, results in

$$h = \frac{2T_s}{T}A_{co} \tag{7}$$

Since the amplitude of A_{co} is unity and T_s/T is the duty ratio of the shoot-through, (7) can be written as,

$$h = 2D \tag{8}$$

From (3) and (8), boost factor B in terms of career shift h is given by

$$B = \frac{1}{1-h} \tag{9}$$

The effect of shoot-through on the modulation index has been illustrated as follows: Modulation index of the system without any shoot-through M_o is given by,

$$M_o = \frac{A_r}{A_{co}} \tag{10}$$

Where A_r is the amplitude of the modulating signal. With the up-shift and down-shift of $h/2$ in a carrier wave, the new amplitude of the carrier wave becomes,

$$A_c = A_{co} \pm \frac{h}{2} \tag{11}$$

The new modulation indices because of up-shift and down-shift of the carrier wave become

$$M_u = \frac{M_o}{A_{co} + \frac{h}{2}} \tag{12}$$

$$M_l = \frac{M_o}{A_{co} - \frac{h}{2}} \tag{13}$$

Now, the average modulation index M can be calculated as

$$M = \frac{M_u\frac{T}{2} + M_l\frac{T}{2}}{T} \tag{14}$$

After simplification,

$$M = \frac{M_o}{1 - \frac{h^2}{4}} \tag{15}$$

The decoupling effect of this control strategy has been verified by evaluating the sensitivity of the boost factor B, and modulation index M, with respect to duty ratio D for SBC and with respect to carrier shift h for SST.

For classical SBC, sensitivity of the boost factor B, and modulation index M with respect to duty ratio D is

$$S_D^B = \frac{\partial B/B}{\partial D/D} = \frac{2D}{(1-2D)} \tag{16}$$

$$S_D^M = \frac{\partial M/M}{\partial D/D} = \frac{-D}{(1-D)} \tag{17}$$

Whereas for proposed SST, sensitivity of the boost factor B and modulation index M with respect to carrier shift h is,

$$S_h^B = \frac{\partial B/B}{\partial h/h} = \frac{h}{(1-h)} \tag{18}$$

$$S_h^M = \frac{\partial M/M}{\partial h/h} = \frac{h^2}{2\left(1-\frac{h^2}{2}\right)} \tag{19}$$

From (16) & (17), it is clear that for SBC, boost factor B and modulation index M are highly sensitive to duty ratio D. From (18) and (19), it is very clear that for proposed SST, sensitivity of the modulation index M with respect to (say for $h = 0.1$) is negligible compared to the sensitivity of boost factor with respect to h. This justifies the decoupling of the modulation index and the boost factor.

The suggested new PWM control strategy has a carrier wave, which is basically, split into two waveforms, and the shift between the two waveforms creates a shoot-through state. These shoot-through states are symmetrical to the active state of SPWM, and preserve the sinusoidal nature of the waveform. This particular way of generating symmetrical shoot-through state has better control in closed loop control as compared to the previous SBC.

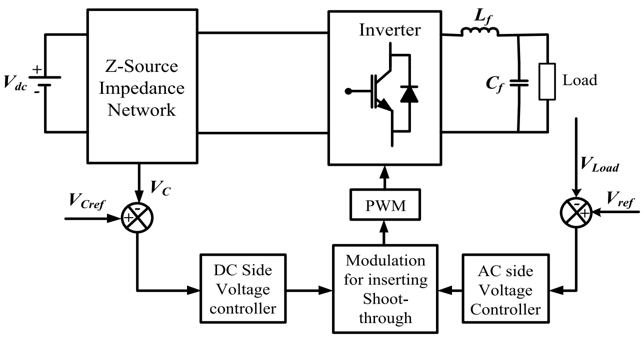

(a)

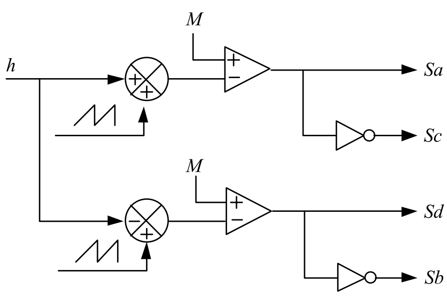

(b)

FIGURE 5. (a) Proposed system control strategy (b) Logic diagram for generation of modulating signal of SST.

IV. CONTROL STRATEGY

The scheme employing AC side control and DC side control is shown in Fig. 5(a). The specifications of the circuit used for the simulation are given in Table 1. As the input DC voltage is of varying nature, the DC side control loop involves the control of DC link voltage in order to maintain a constant voltage across the inverter. The Z-source capacitor voltage needs to be regulated in order to regulate the DC link voltage, which would be input to the inverter. For variations in input DC voltage, the DC link voltage will vary, and accordingly, the load voltage will vary. Thus, the DC link voltage must be regulated. For this, the Z-source capacitor voltage is taken as the controlling quantity. This voltage is compared with a reference value, and this error quantity is fed to the PI controller, which eventually, generates the modulation signal for inserting the shoot-through in, the zero states. Thus, the DC link voltage is controlled effectively, by modulation of the shoot-through duty ratio. The AC side control loop involves the control of AC side voltage with reference generation for generating the modulating signal. This control involves a comparison of the output voltage with, a reference voltage, and this compared output is fed to a PI controller, which in turn, generates the modulating signal for the generation of PWM signals.

TABLE 1. Specifications of ZS.

Parameters	Values
Output Voltage	$V_L = 110$ V rms
Supply Frequency	$f = 50$ Hz
Switching Frequency	$f_{sw} = 10$ kHz
AC side inductor	$L_f = 2.2$ mH
AC side capacitor	$C_f = 5$ µF
Z-Source inductor	$L_1 = L_2 = L = 160$ µH
Z-Source Capacitor	$C_1 = C_2 = C = 1000$ µF
Load Power	$P_L = 300$ W

The logic diagram for the generation of a modulating signal is shown in Fig. 5(b). The DC side controller, provides the shift in a carrier wave by h and the AC side controller, provides the modulating signal is represented by M. The two carrier signal is upward and downward shifted by $h/2$ value using the summing amplifier. Upward shifted carrier is compared with modulating signal to produce a PWM signal of first leg upper switching device S_a and the complement of this signal provide the PWM signal of second leg upper switching device S_c. Similarly, downward shifted carrier waveform is compared with a modulating signal to produce PWM signals of lower switching devices S_d and S_b. This shifted carrier approach produces the necessary shoot-through states logically.

V. SIMULATION RESULTS

Simulation of the proposed system has been carried out in the SIMULINK software. The simulation results of closed loop control with a carrier and a reference signal under different zooming conditions are shown in Fig. 6. Two carrier waves and one reference sinusoidal wave are shown in Fig. 6(a). More clarity can be obtained from a zoomed version shown

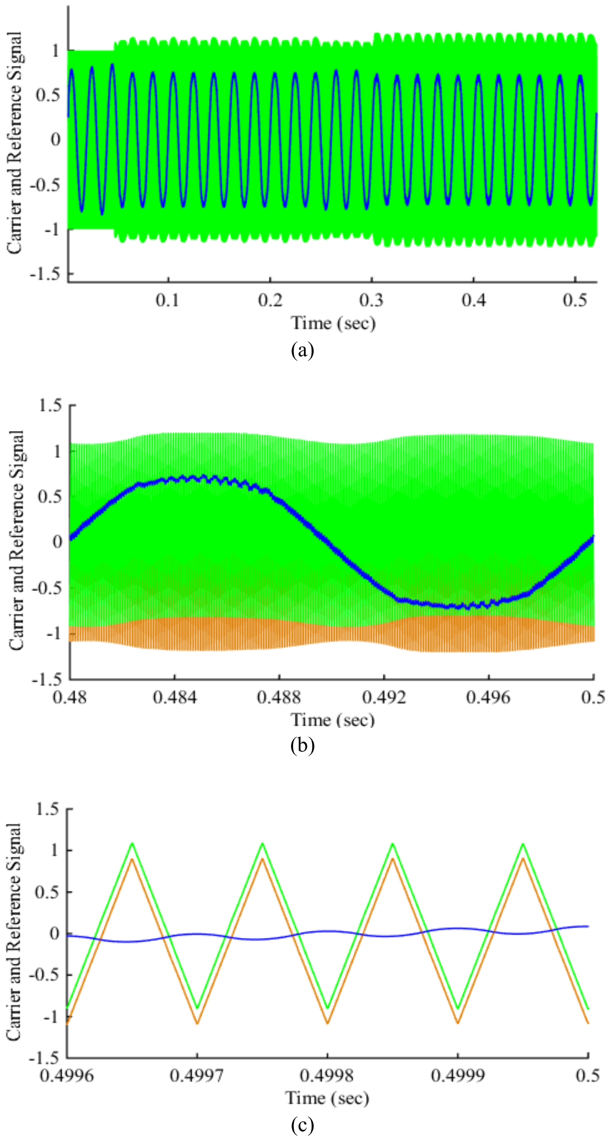

FIGURE 6. Waveforms of carrier and reference waves under different zooming conditions.

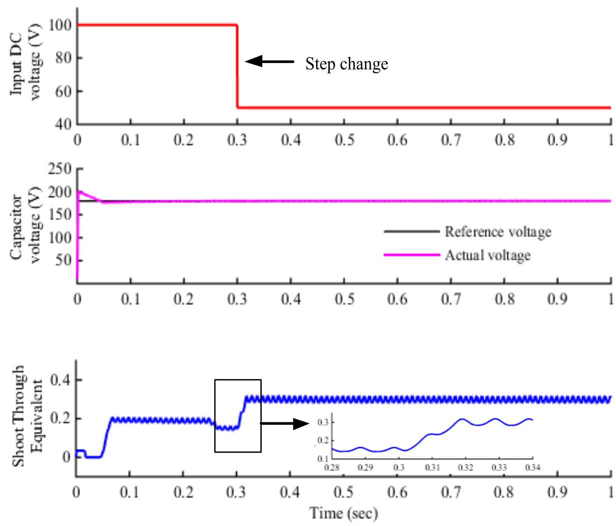

FIGURE 7. Waveforms showing DC side control with step change in input voltage.

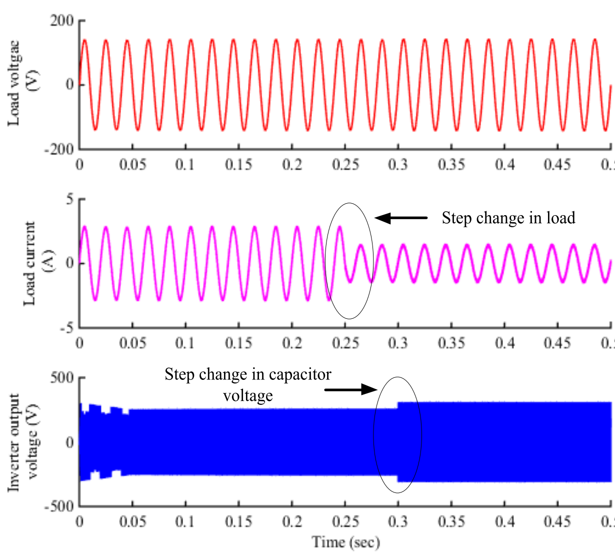

FIGURE 8. Waveforms showing AC side control with step change in load (0.25 sec), followed by small step change in reference capacitor voltage (0.3 sec).

in Fig. 6(b) and Fig. 6(c). The up-shift and down-shift in carrier waves result in a shoot-through state as explained before. The newly proposed method, logically incorporates the shift in the carrier to produce the required shoot through. So the ripple in carrier wave is because of change in shoot-through signal for the DC side controller. This carrier signal variation is to be provided in certain limits (maximum of 0.4) and is only proposed for Z-source topologies, where the shoot-through states appears.

Fig. 8, shows the effectiveness of the DC side control and AC side control. To demonstrate the effectiveness of the AC side control, a step change in load at 0.25 sec has been introduced. This step change in load is followed by a small step rise in the reference capacitor voltage at 0.3 sec, which demonstrates the effectiveness of DC side control. A step change in the reference value of capacitor voltage from 250V to 300V is applied at 0.3 sec. The DC side controller is fast enough to regulate the capacitor voltage from 250V to 300V within few milliseconds. Also, the effect of this capacitor voltage change is negligible on AC side voltage and current waveforms.

Therefore, the proposed control strategy, in terms of SST is proven to be effective on both the DC and AC side. However, some constraint has to be put on the value of h to allow this method to function effectively.

Further, harmonic analysis is carried out in order to prove the efficacy, of the proposed method in terms of reduced, harmonic, and decoupled control. While carrying out the harmonic analysis for comparison purposes, the modulation

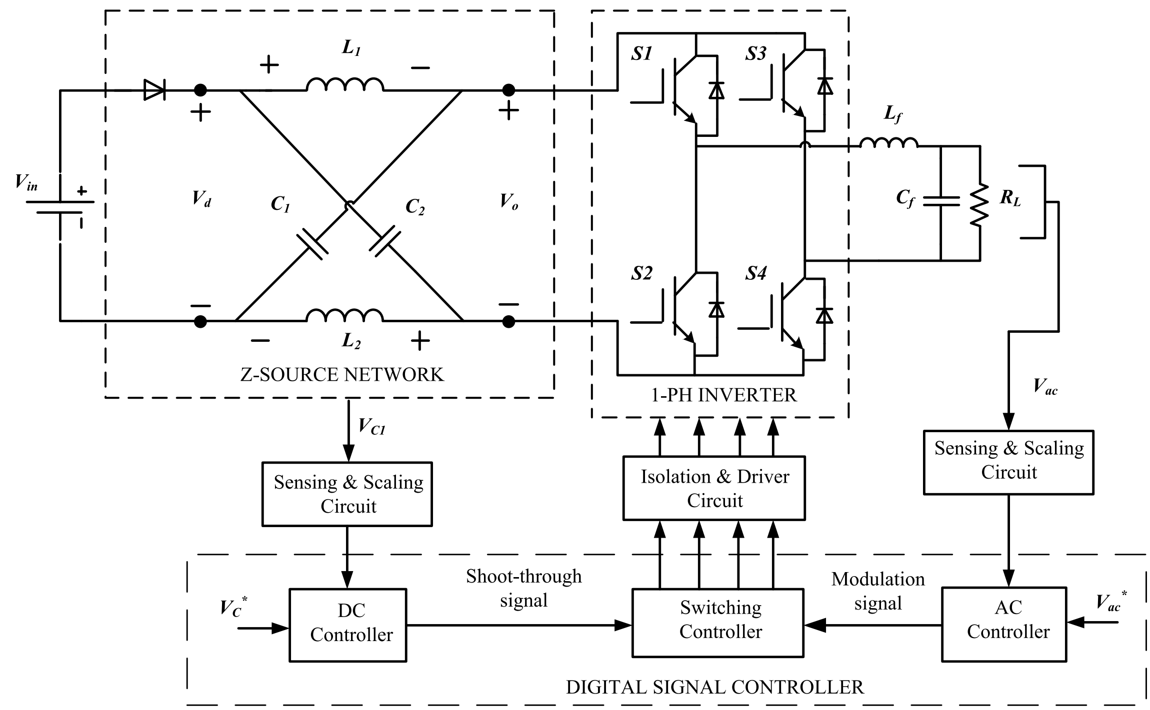

FIGURE 9. Schematic of the hardware setup of proposed system.

index and shoot-through duty cycle are independently controlled. The modulation index is to be varied in accordance with the output voltage control and therefore, it is adjusted so as to get fixed AC output voltage for the analysis. The shoot-through duty ratio is varied in accordance with different values of the reference capacitor voltages, and the harmonics in the output voltage and current profile are analyzed.

TABLE 2. Harmonic analysis of simple boost control (SBC).

Sr. No.	AC output voltage (V_o) rms	Reference capacitor voltage (V_c) Volt	THD of Current (%)	THD of Voltage (%)
1	110	150	15.72	0.91
2	110	180	16.03	0.97
3	110	200	20.28	1.13
4	110	250	13.24	0.39

The THD results of SBC and SST, presented in Table 2 and Table 3 respectively, are derived for different values of the reference capacitor voltage 150V, 180V, 200V, and 250V thereby, adjusting the duty ratios. It is clear that the THD of SST is very less as compared to SBC.

Overall, it is seen that SST is more feasible as compared to SBC. In SBC, the capacitor voltage control is limited to the particular value, but in SST it is not limited and therefore, there is a scope of the controlling capacitor voltage, over a large range. As harmonics are less, the rating of the inductor decreases. This further decreases the overall cost of the system, thus, making it economical, and more efficient.

TABLE 3. Harmonic analysis of symmetrical shoot-through control (SST).

Sr. No.	AC output voltage (V_o) rms	Reference capacitor voltage (V_c) Volt	THD of Current (%)	THD of Voltage (%)
1	110	150	1.03	1.06
2	110	180	1.10	1.11
3	110	200	1.06	1.08
4	110	250	1.77	1.86

*Input DC voltage = 100V

VI. EXPERIMENTAL STUDY

The schematic of hardware setup of proposed system is shown in Fig. 9. The output of the controlled DC source is connected at the input of the Z-source impedance network. Z-source impedance network is connected to single-phase H-bridge inverter. DC capacitor voltage and AC inverter output voltage signals are connected to the ADC channels of the controller through scaling and the signal conditioning circuit. Capacitor voltage is compared with internal capacitor voltage reference value, and this error signal is fed to the DC side controller. The output of the DC side controller produces the shoot-through signal h. Inverter output voltage is compared with internal reference AC voltage, and this error signal is fed to the AC side controller. The output of the AC side controller produces the modulating signal M. These two signals, shoot-through signal h and modulating signal M, are used to produce symmetrical shoot-through PWM signals. PWM output

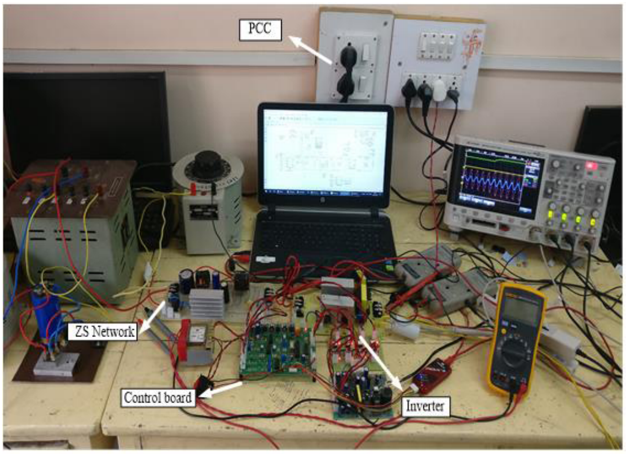

FIGURE 10. Hardware setup of the complete system.

pins of the controller are connected to the inverter switches through an isolation and driver circuit.

The photograph of experimental setup for hardware implementation of the proposed system is shown in Fig. 10. A prototype of 300W rating has been implemented in the laboratory. The output of the inverter is designed for 110V, 50Hz and the switching frequency is set at 10kHz. A resistive load is connected across the inverter to verify steady state and a dynamic response of the overall system.

A 16-bit fixed point low-cost digital controller, dsPIC33EP64MC202 has been used for DC and AC side control loop realization, and gating pulse generation. This digital controller has 12-bit ADC, and a high-resolution PWM module, which makes it suitable for such type of power electronics based real-time applications. The digital controller is set to operate at a system clock frequency of 60MHz. IRF460 MOSFET switches have been used as inverter switches along with TLP250 as the isolation and gate driving circuit.

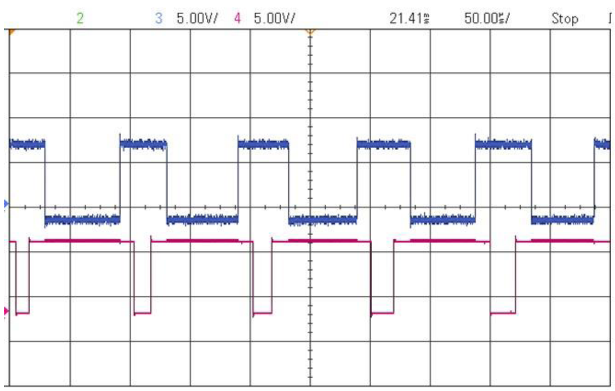

FIGURE 11. Symmetrical shoot-through PWM of one leg of inverter (Inverter switches Sa and Sb).

Fig. 11, shows the PWM pulses that are to be applied to the gate of the two MOSFET switches of a single leg of the inverter. These PWM waveforms show the symmetrically

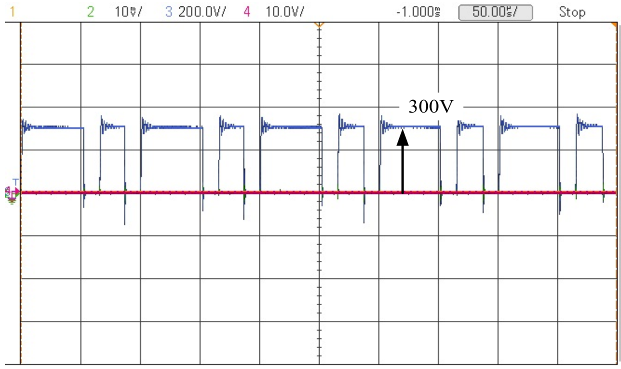

FIGURE 12. Inverter input DC voltage.

distributed shoot-through states, across each pulse of the active period. As claimed earlier, the sinusoidal nature of the switching pattern is preserved here. Fig. 12, shows inverter input DC voltage. During the shoot-through states inverter input DC voltage is zero, and during non-shoot-through states inverter input DC voltage is $(2V_c - V_{in})$.

TABLE 4. Experimental results of harmonic content for symmetrical shoot-through control.

Sr. No.	A.C output voltage (V_o) rms	Reference capacitor voltage (V_c) Volt	THD of Current (%)	THD of Voltage (%)
1	110	150	4.33	3.52
2	110	180	4.78	3.85

*Input DC voltage = 120V

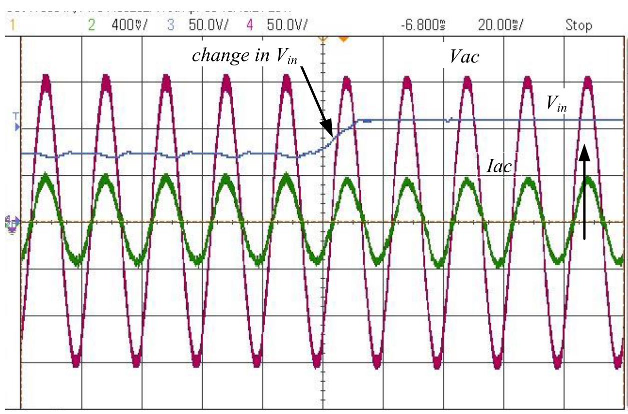

FIGURE 13. Experimental results for step change in input voltage from 80V to 120V (at capacitor reference voltage of 150V).

The experimental results of the harmonic content of the proposed system are presented in Table 4. The effect of a step change in input voltage can be observed from Fig. 13. Initially, DC voltage of 80V is applied to the input of the impedance network, while the capacitor voltage is regulated at 150V, and the output voltage is regulated at 110V rms. A step change in input voltage from 80V to 120V is applied to verify, the effectiveness of the DC and AC side controller. It is seen that even after a step change in the input voltage of 50%, the AC side voltage and current remains regulated.

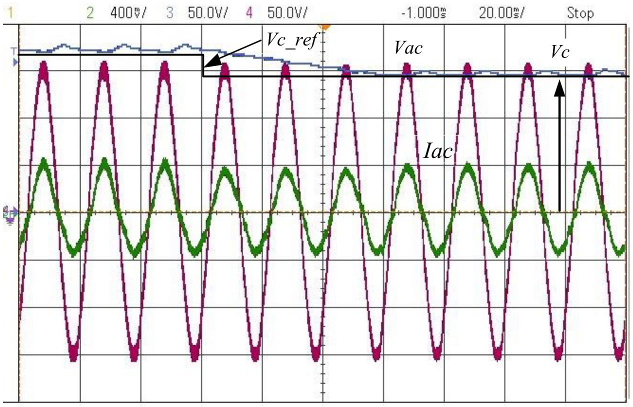

FIGURE 14. Experimental results for step change in reference capacitor voltage from 180V to 150V (at input voltage of 120V).

The waveforms of the output voltage and the current of the inverter for a step change in capacitor reference voltage is observed in Fig. 14. Keeping the input voltage constant at 120V and AC output voltage at 110V, a step change in capacitor voltage is applied from 180V to 150V. What is depicted from the figure is that the AC side control is fast enough to keep output voltage and hence, the load current is at a constant value.

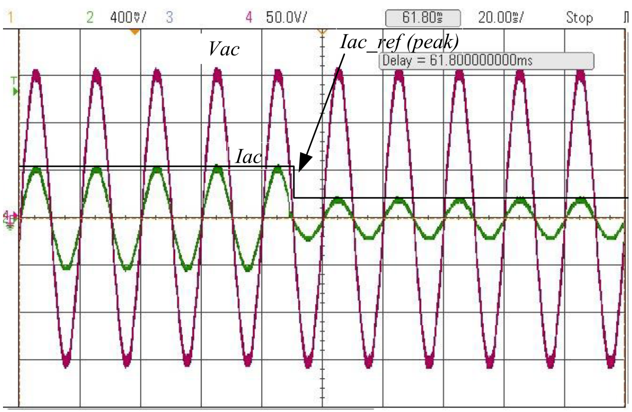

FIGURE 15. Experimental results for step change in load from 2.5A to 1A (at input voltage 100V and capacitor reference voltage at 150V).

Furthermore, a step change in load current from 2.5A to 1A is applied to demonstrate the dynamic response of the AC side controller as visualized in Fig. 15.

Thus, the experimental results validate the simulation performance of the control in terms of input voltage variations, changes in capacitor reference voltage, and load current variations. This proves the efficacy, of the proposed controller.

VII. CONCLUSION

A novel PWM method for a Z-Source Inverter with symmetrical shoot-through states is presented in this paper. It is found from the simulation results that, when decoupled control is investigated, the total harmonic distortion is lesser as compared to the existing PWM methods presented in the literature. This paper also demonstrates, a simple carrier shifting method for the implementation of this symmetrical shoot-through PWM. Both, the simulation and experimental results are presented to demonstrate the efficacy, of the proposed technique. The dynamic response of the controller with the proposed PWM is validated over wider operating conditions. Moreover, this method can be extended to the other variants of a Z-Source Inverter like the Quasi-Z-Source Inverter.

REFERENCES

[1] F. Z. Peng, "Z-source inverter," *IEEE Trans. Ind. Appl.*, vol. 39, no. 2, pp. 504–510, Mar./Apr. 2003.

[2] F. Z. Peng, M. Shen, and Z. Qian, "Maximum boost control of the Z-source inverter," *IEEE Trans. Power Electron.*, vol. 20, no. 4, pp. 833–838, Jul. 2005.

[3] C. J. Gajanayake, F. L. Luo, H. B. Gooi, P. L. So, and L. K. Siow, "Extended-boost *Z*-source inverters," *IEEE Trans. Power Electron.*, vol. 25, no. 10, pp. 2642–2652, Oct. 2010.

[4] M. Zhu, K. Yu, and F. L. Luo, "Switched inductor Z-source inverter," *IEEE Trans. Power Electron.*, vol. 25, no. 8, pp. 2150–2158, Aug. 2010.

[5] P. C. Loh, F. Blaabjerg, and C. P. Wong, "Comparative evaluation of pulsewidth modulation strategies for Z-source neutral-point-clamped inverter," *IEEE Trans. Power Electron.*, vol. 22, no. 3, pp. 1005–1013, May 2007.

[6] Z. J. Zhou, X. Zhang, P. Xu, and W. X. Shen, "Single-phase uninterruptible power supply based on Z-source inverter," *IEEE Trans. Ind. Electron.*, vol. 55, no. 8, pp. 2997–3004, Aug. 2008.

[7] C. J. Gajanayake, D. M. Vilathgamuwa, P. C. Loh, R. Teodorescu, and F. Blaabjerg, "Z-source-inverter-based flexible distributed generation system solution for grid power quality improvement," *IEEE Trans. Energy Convers.*, vol. 24, no. 3, pp. 695–704, Sep. 2009.

[8] K. Patidar and A. C. Umarikar, "High step-up pulse-width modulation DC–DC converter based on quasi-Z-source topology," *IET Power Electron.*, vol. 8, no. 4, pp. 477–488, 2015.

[9] S. A. Singh, N. A. Azeez, and S. S. Williamson, "A new single-stage high-efficiency photovoltaic (PV)/grid-interconnected DC charging system for transportation electrification," in *Proc. 41st Annu. Conf. IEEE Ind. Electron. Soc. (IECON)*, Jun. 2015, pp. 5374–5380.

[10] G. Buja, R. K. Keshri, and R. Menis, "Comparison of DBI and ZSI supply for PM brushless DC drives powered by fuel cell," in *Proc. IEEE Int. Symp. Ind. Electron.*, Jul. 2011, pp. 165–170.

[11] D. M. Vilathgamuwa, C. J. Gajanayake, and P. C. Loh, "Modulation and control of three-phase paralleled Z-source inverters for distributed generation applications," *IEEE Trans. Energy Convers.*, vol. 24, no. 1, pp. 173–183, Mar. 2009.

[12] G. L. Cazlo, A. Lidozzi, L. Solero, and F. Crescimbini, "Three-phase Z-source power supply design," *IET Power Electron.*, vol. 5, no. 8, pp. 1270–1281, 2012.

[13] Y. Tang, S. Xie, and C. Zhang, "Single-phase z-source inverter," *IEEE Trans. Power Electron.*, vol. 26, no. 12, pp. 3869–3873, Dec. 2011.

[14] Y. Liu, B. Ge, H. Abu-Rub, and D. Sun, "Comprehensive modeling of single-phase quasi-Z-source photovoltaic inverter to investigate low-frequency voltage and current ripple," *IEEE Trans. Ind. Electron.*, vol. 62, no. 7, pp. 4194–4202, Jul. 2015.

[15] Q. V. Tran, T. W. Chun, J. R. Ahn, and H. H. Lee, "Algorithms for controlling both the DC boost and AC output voltage of Z-source inverter," *IEEE Trans. Ind. Electron.*, vol. 54, no. 5, pp. 2745–2750, Oct. 2007.

[16] M. S. Diab, A. A. Elserougi, A. M. Massoud, A. S. Abdel-Khalik, and S. Ahmed, "A pulsewidth modulation technique for high-voltage gain operation of three-phase Z-source inverters," *IEEE J. Emerg. Sel. Topics Power Electron.*, vol. 4, no. 2, pp. 521–533, Jun. 2016.

[17] Y. Tang, S. Xie, C. Zhang, and Z. Xu, "Improved Z-source inverter with reduced Z-source capacitor voltage stress and soft-start capability," *IEEE Trans. Power Electron.*, vol. 24, no. 2, pp. 409–415, Feb. 2009.
[18] S. A. Singh, N. A. Azeez, and S. S. Williamson, "Capacitance reduction in a singlephase quasi-Z-source inverter using a hysteresis current controlled active power filter," in *Proc. 25th IEEE Int. Symp. Ind. Electron. (ISIE)*, Apr. 2016, pp. 805–810.
[19] S. Dalapati and C. Chakraborty, "A direct PWM technique for a single-phase full-bridge inverter through controlled capacitor charging," *IEEE Trans. Ind. Electron.*, vol. 55, no. 8, pp. 2912–2922, Aug. 2008.
[20] A. Ravindranath, S. K. Mishra, and A. Joshi, "Analysis and PWM control of switched boost inverter," *IEEE Trans. Ind. Electron.*, vol. 60, no. 12, pp. 5593–5602, Dec. 2013.

SUMANT G. KADWANE (SM'16) received the B.E. degree in electrical engineering from Yeshwantrao Chavan College of Engineering (Y.C.C.E.), Nagpur University, Nagpur, India, the M.E. degree in control systems from the Government College of Engineering at Pune, Pune University, and the Ph.D. degree in engineering from the Birla Institute of Technology, Mesra, India. He was a Faculty Member with the Department of EEE, BIT, Mesra, for seven years. He is currently a Professor with the Department of Electrical Engineering, Yeshwantrao Chavan College of Engineering, Nagpur, India, where he is teaching both undergraduate and postgraduate students. He has guided over 25 postgraduate students with various control and DSP-based projects. His areas of interest are control system design, power electronic converters, and renewable energy. He is a member of IE(I) and ISTE. He is Editor-in-Chief of the *Journal for Research in Engineering and Applied Sciences*.

UMESH K. SHINDE received the B.E. degree in electrical engineering from the Government College of Engineering at Karad, Shivaji University, Kolhapur, India, and the M.E. degree in control systems from the Government College of Engineering at Pune, Pune University. He is currently pursuing the Ph.D. degree with Yeshwantrao Chavan College of Engineering, Nagpur, India. He has 13 years of teaching experience and three years of industrial experience, and he is currently an Assistant Professor with the Department of Electrical Engineering, Bhivarabai Sawant College of Engineering and Research, Pune, India. His areas of interest are power electronic converters and renewable energy.

SNEHAL P. GAWANDE (M'16) received the B.E. degree in electrical engineering and the M.Tech. degree in integrated power systems from Nagpur University and the Ph.D. degree from V.N.I.T., Nagpur, India. He has 13 years of teaching experience and is currently an Assistant Professor with the Department of Electrical Engineering, Yeshwantrao Chavan College of Engineering, Nagpur. He authored over 50 papers published in reputed peer-reviewed journals, such as IEEE Transactions, IET, and Elsevier and IEEE conferences, such as PEDES, IECON, PESC, and INDICON. His research interests include power electronics, FACTS, power quality, and power electronics applications to renewable energy systems. He is a Life Member of ISTE and IACSIT and a member of the Institution of Engineers, India. He is a regular Reviewer of IEEE Transactions, IET, Elsevier, and Taylor and Francis and for various reputed IEEE conferences, such as PEDES, IECON, CIGRE, and PES Winter meetings. He is an Editor of the *Journal of Electrical and Power System Engineering*, *Journal of Advances in Electrical Drives*, and *Journal of Controller and Converters*.

RITESH KUMAR KESHRI received the bachelor's and master's degrees from NIT Jamshedpur, India, and the Ph.D. degree from the University of Padova, Italy. He was an Assistant Professor with BIT Mesra, Ranchi, India, from 2006 to 2015. He is currently with the Department of Electrical Engineering, Visvesvaraya National Institute of Technology, Nagpur, India, as an Assistant Professor. His research interests include power electronics and electric drives for electric vehicle propulsion and renewable. He received the Silver Medal for being first in M.Tech. (electrical) in 2007, the Young Researcher Fellowship from the Ministry of University of Italy in 2008, the Erasmus Mundus Fellowship for Ph.D. from the European Union in 2010, a First Prize as a Student Team Leader of the University of Padova in class-3 of Formula Electric and Hybrid in 2011, and the 2016 Best Paper Award of the IEEE Transactions on Industrial Electronics. He is associated with the IEEE-IES and IEEE-PELS, and has been contributing as organizing chairs for technical track and special sessions of IECON since 2013. He was the Chair for Conference Activities for the Technical Committee on Transportation Electrification (TCTE) of the IEEE Industrial Electronics Society from 2014 to 2015, and is the Secretary of TCTE-IES and the Chair of the Sub-Committee for EV/HEV/FCEV of TCTE.